8 Greer CE, Lund JK, Manos MM. PCR amplification from paraffin-embedded tissues: Recommendations on fixatives for long-term storage and prospective studies. *PCR Methods Appl* 1991; **1**: 46–50.
9 Wolff AC, Hammond ME, Schwartz JN *et al.* American Society of Clinical Oncology/College of American Pathologists guideline recommendations for human epidermal growth factor receptor 2 testing in breast cancer. *Arch Pathol Lab Med* 2007; **131**: 18–43.
10 Wolff AC, Hammond ME, Schwartz JN *et al.* American Society of Clinical Oncology/College of American Pathologists guideline recommendations for human epidermal growth factor receptor 2 testing in breast cancer. *J Clin Oncol* 2007; **25**: 118–45.
11 Dowsett M, Nielsen TO, A'Hern R *et al.* Assessment of Ki67 in breast cancer: Recommendations from the International Ki67 in Breast Cancer working group. *J Natl Cancer Inst* 2011; **103**: 1656–64.
12 Nakhleh RE, Grimm EE, Idowu MO *et al.* Laboratory compliance with the American Society of Clinical Oncology/college of American Pathologists guidelines for human epidermal growth factor receptor 2 testing: A College of American Pathologists survey of 757 laboratories. *Arch Pathol Lab Med* 2010; **134**: 728–34.
13 Hewitt SM, Lewis FA, Cao Y *et al.* Tissue handling and specimen preparation in surgical pathology: Issue concerning the recovery of nucleic acids from formalin-fixed, paraffin-embedded tissue. *Arch Pathol Lab Med* 2008; **132**: 1929–35.
14 Renne R, Fouillet X, Maurer J *et al.* Recommendation of optimal method for formalin of rodent lungs in routine toxicology studies. *Toxicol Pathol* 2001; **29**: 587–9.
15 Nofech-Mozes S, Vella ET, Dhesy-Thind S *et al.* Cancer care ontario guideline recommendations for hormone receptor testing in breast cancer. *Clin Oncol* 2012; **24**: 684–96.
16 Summary of ASCO/CAP HER2 Guideline Recommendations. (Accessed 6 September 2011.) Available from: http://www.cap.org/apps/docs/committees/immunohistochemistry/summary_of_recommendations.pdf
17 CAP Home. KRAS Mutation Testing for Colorectal Cancer (CRC). (Accessed 17 December 2010.) Available from: http://www.cap.org/apps/cap.portal
18 CAP Home. Frequently Asked Questions About ER/PgR Testing Guidelines. (Accessed 12 January 2011.) Available from: http://www.cap.org/apps/cap.portal
19 Preusser M, Heinzl H, Gelpi E *et al.* Ki67 index in intracranial ependymoma: A promising histopathological candidate biomarker. *Histopathology* 2008; **53**: 39–47.
20 Ludyga N, Grünwald B, Azimzadeh O *et al.* Nucleic acids from long-term preserved FFPE tissues are suitable for downstream analyses. *Virchows Arch* 2012; **460**: 131–40.
21 Takano EA, Mikeska T, Dobrovic A *et al.* A multiplex endpoint RT-PCR assay for quality assessment of RNA extracted from formalin-fixed paraffin-embedded tissues. *BMC Biotechnol* 2010; **10**: 89.
22 Engel KB, Moore HM. Effects of preanalytical variables on the detection of proteins by immunohistochemistry in formalin-fixed, paraffin-embedded tissue. *Arch Pathol Lab Med* 2011; **135**: 537–43.
23 Arber DA. Effect of prolonged formalin fixation on the immunohistochemical reactivity of breast markers. *Appl Immunohistochem Mol Morphol* 2002; **10**: 183–6.
24 Srinivasan M, Sedmak D, Jewell S. Effect of fixatives and tissue processing on the content and integrity of nucleic acids. *Am J Pathol* 2002; **161**: 1961–71.
25 Staff S, Kujala P, Karhu R *et al.* Preservation of nucleic acids and tissue morphology in paraffin-embedded clinical samples: Comparison of five molecular fixatives. *J Clin Pathol* 2013; **66**: 807–10.
26 Groelz D, Sobin L, Branton P *et al.* Non-formalin fixative versus formalin-fixed tissue: A comparison of histology and RNA quality. *Exp Mol Pathol* 2013; **94**: 188–94.
27 Milcheva R, Janega P, Celec P *et al.* Alcohol based fixatives provide excellent morphology, protein immunoreactivity and RNA integrity in paraffin embedded tissue specimens. *Acta Histochem* 2013; **115**: 279–115. Available online 24 August 2012.

SUPPORTING INFORMATION

Additional Supporting Information may be found in the online version of this article at the publisher's web-site:

Table S1 The primer sequences information.

© 2014 The Authors
Pathology International © 2014 Japanese Society of Pathology and Wiley Publishing Asia Pty Ltd

European Journal of Cancer (2014) 50, 1900–1908

Available at www.sciencedirect.com

ScienceDirect

journal homepage: www.ejcancer.com

Prognostic impact of M2 macrophages at neural invasion in patients with invasive ductal carcinoma of the pancreas

Motokazu Sugimoto [a,b,d], Shuichi Mitsunaga [a,c], Kiyoshi Yoshikawa [a], Yuichiro Kato [b], Naoto Gotohda [b], Shinichiro Takahashi [b], Masaru Konishi [b], Masafumi Ikeda [c], Motohiro Kojima [a], Atsushi Ochiai [a,*], Hironori Kaneko [d]

[a] *Division of Pathology, Research Center for Innovative Oncology, National Cancer Center Hospital East, Japan*
[b] *Department of Hepatobiliary and Pancreatic Surgery, National Cancer Center Hospital East, Japan*
[c] *Department of Hepatobiliary and Pancreatic Oncology, National Cancer Center Hospital East, Japan*
[d] *Department of Surgery, Toho University School of Medicine, Japan*

Received 11 March 2014; accepted 9 April 2014
Available online 15 May 2014

KEYWORDS
Pancreatic cancer
Pancreaticoduodenectomy
Neural invasion
M2 macrophages
Overall survival
Peritoneal dissemination
Locoregional recurrence
Adjuvant chemotherapy

Abstract ***Background:*** Neural invasion is a characteristic pattern of invasion and an important prognostic factor for invasive ductal carcinoma (IDC) of the pancreas. M2 macrophages have reportedly been associated with poor prognosis in various cancers. The aim of the present study was to investigate the prognostic impact of M2 macrophages at extrapancreatic nerve plexus invasion (plx-inv) of pancreatic IDC.

Methods: Participants comprised 170 patients who underwent curative pancreaticoduodenectomy for pancreatic IDC. Immunohistochemical examination of surgical specimens was performed by using CD204 as an M2 macrophage marker, and the area of immunopositive cells was calculated automatically. Prognostic analyses of clinicopathological factors including CD204-positive cells at plx-inv were performed.

Results: Plx-inv was observed in 91 patients (53.5%). Forty-eight patients showed a high percentage of CD204-positive cell area at plx-inv (plx-inv CD204%^{high}). Plx-inv CD204%^{high} was an independent predictor of poor outcomes for overall survival (OS) ($P < 0.001$) and disease-free survival (DFS) ($P < 0.001$). Patients with plx-inv CD204%^{high} showed a shorter time to peritoneal dissemination ($P < 0.001$) and locoregonal recurrence ($P < 0.001$). In patients who underwent adjuvant chemotherapy, plx-inv CD204%^{high} was correlated with shorter OS ($P = 0.011$) and DFS ($P = 0.038$) in multivariate analysis.

* *Corresponding author:* Address: National Cancer Center Hospital East, 6-5-1 Kashiwa-no-ha, Kashiwa, Chiba 277-8577, Japan. Tel.: +81 4 7134 6855; fax: +81 4 7134 6865.
E-mail address: aochiai@east.ncc.go.jp (A. Ochiai).

http://dx.doi.org/10.1016/j.ejca.2014.04.010
0959-8049/© 2014 Elsevier Ltd. All rights reserved.

Conclusions: Plx-inv CD204%^{high} was associated with shortened OS and DFS and early recurrence in the peritoneal cavity and locoregional space. The prognostic value of plx-inv CD204%^{high} was also applicable to patients who received adjuvant chemotherapy. High accumulation of M2 macrophages at plx-inv represents an important predictor of poor prognosis.

© 2014 Elsevier Ltd. All rights reserved.

1. Introduction

Pancreatic cancer is an aggressive malignancy with a high incidence of recurrence and low rates of survival, even when curative resection is achieved [1,2]. However, the mechanisms underlying this intractability have yet to be elucidated. Neural invasion has been accepted as an important prognostic factor for invasive ductal carcinoma (IDC) of the pancreas [3–7]. Patients with severe neural invasion are categorised as unresectable cases [8] and experience pain, cachexia, peritoneal dissemination and poor prognosis [9–11].

In vivo and *in vitro* models have been established to shed light on the mechanisms underlying neural invasion [9,12–15]. In our previous study [12], highly expressed genes in nerve tissues of the mouse model using Capan-1, a human pancreatic cancer cell line, included macrophage-related genes such as lysozyme [16], macrophage-expressed gene 1 glycoprotein [16] and early growth response 1 [17]. In other experimental studies, the paracrine regulation of neurotrophins was associated with the recruitment of macrophages in neural invasion and the migration of tumour cells [14,15]. Accumulation of macrophages at sites of neural invasion is considered to support tumour cell proliferation and is presumably related to poor prognosis.

Macrophages that have infiltrated into cancer stroma are termed tumour-associated macrophages (TAMs) and promote tumour progression and metastasis [18]. Increased density of TAMs is associated with poor prognosis in cancers of the thyroid, prostate, stomach, bile duct and pancreas [19–23]. TAMs express an M2-skewed phenotype, which is activated in chronic inflammation, scavenge debris and promote angiogenesis and tissue remodelling [18]. M2 macrophages show high expression of scavenger receptor (SR)-A (CD204). High accumulation of CD204-positive cells at the periphery of pancreatic IDC was correlated with shorter overall survival (OS) and disease-free survival (DFS) in our previous study [23]. However, to the best of our knowledge, the clinical impact of M2 macrophages in neural invasion sites has not been elucidated in any kind of malignancies. The aim of the present study was to investigate the prognostic value of M2 macrophages at neural invasion in patients with pancreatic IDC who underwent curative pancreaticoduodenectomy.

2. Methods

2.1. Patients

A total of 177 patients underwent curative (R0) pancreaticoduodenectomy and were histologically diagnosed with pancreatic IDC at our institution between September 1992 and June 2011. Seven patients were excluded due to surgical mortality ($n = 3$), incomplete follow-up data ($n = 2$) and poor-quality surgical specimens ($n = 2$). The remaining 170 patients were included in this investigation. The median patient age at the time of surgery was 65 years [range, 34–84 years], and 63 (37.1%) were women. Sixty patients received postoperative adjuvant chemotherapy, consisting of gemcitabine in 40 patients (66.7%), S-1 (an oral fluoropyrimidine) in 10 (16.7%), gemcitabine plus S-1 in 6 (10.0%) and 5-fluorouracil plus cisplatin in 4 (6.7%). Inclusion criteria for adjuvant chemotherapy basically conformed to the criteria of the nationwide Japanese randomised phase III trial [24]. Neoadjuvant therapy was performed in four patients. Lymphadenectomy was performed according to the Japanese General Rules for the Study of Pancreatic Cancer [25]. All patients signed an institutional review board-approved informed consent form.

2.2. Evaluation of clinicopathological features

Each resected specimen was fixed in 10% formalin at room temperature, and the size and gross appearance of the tumour were recorded [3]. The entire tumour was cut at intervals of 0.5–0.7 cm, and the specimens were routinely processed and embedded in paraffin. Serial sections (3-μm thick) of each tumour were cut, and one section was stained with haematoxylin and eosin (HE). Histopathological findings were examined according to the definitions of the Japan Pancreas Society [25]. The following clinicopathological factors were investigated to assess their prognostic value: age; sex; Eastern Cooperative Oncology Group performance status (ECOG PS); presence of adjuvant chemotherapy; serum level of carcinoembryonic antigen (CEA); serum level of carbohydrate antigen (CA)19-9; tumour differentiation; tumour size; serosal invasion; retroperitoneal invasion; portal vein invasion; lymphatic invasion (ly); vessel invasion (v); intrapancreatic neural invasion (ne); lymph node involvement and extrapancreatic nerve plexus invasion

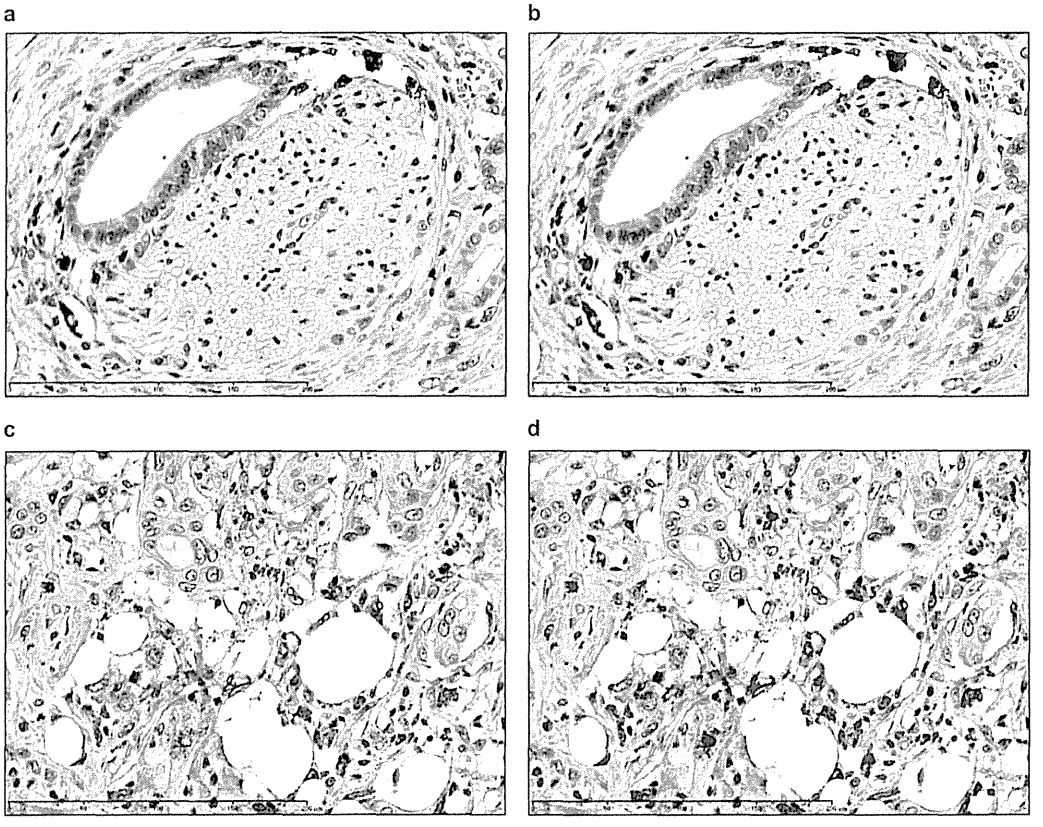

Fig. 1. (a) CD204-positive cells at an extrapancreatic nerve plexus invasion (plx-inv) (magnification, ×400). (b) Red areas represent CD204-positive cells, and the percentage area of CD204-positive cells was calculated as (area of CD204-positive cells/measured area) × 100 using the automeasure function in Axio Vision 4.7.1 software (Carl Zeiss, Oberkochen, Germany). (c) CD204-positive cells at the tumour periphery (magnification, ×400). (d) CD204-positive cells are expressed as red areas.

(plx-inv). Ly, v and ne were classified into four groups based on the most extensively involved area observed under low-power magnification (×100): no invasion of cancer cells; slight invasion of a few cancer cells (1–3 points); moderate invasion (4–8 points) and severe invasion (>8 points). Pathological stage was evaluated according to the 7th edition of the International Union Against Cancer (UICC) classification (IA/IB/IIA versus IIB/III/IV) [26]. Cut-off values for continuous variables were determined from median values for all patients.

2.3. Definition of the tumour periphery and plx-inv

HE-stained sections at the maximal diameter of the tumour were evaluated at a magnification of ×40, and the margin of the tumour was marked on each slide. The periphery of the primary tumour was defined as fields that included cancer cells and adjacent non-cancerous cells at a magnification of ×100 [23]. As described in our previous study [3], plx-inv was defined as invasion of tumour cells inside the perineurium, apart from both the pancreatic capsule and main tumour, and was evaluated at a magnification of ×400 in all sections. Plx-inv distance was defined as the distance from the plx-inv to the main tumour. The cut-off for plx-inv distance was set at 2500 μm, and the prognostic value was evaluated [3].

2.4. Immunohistochemical staining and evaluation

Mouse anti-human CD204 antibody (Scavenger Receptor class A-E5, 1:400 in blocking buffer; Transgenic, Kumamoto, Japan) was used for immunohistochemical staining [23]. The percentage area of CD204-positive cells (CD204%) was calculated as (area of CD204-positive cells/measured area) × 100 using the automeasure function in Axio Vision 4.7.1 software (Carl Zeiss, Oberkochen, Germany) [23]. The mean CD204% for three hot spots at the tumour periphery and plx-inv was calculated in each patient. Median CD204% for all patients with plx-inv was used to determine CD204%^{high} as equal to or above the median. Prognostic analyses for CD204%^{high} at the periphery and plx-inv were performed.

2.5. Assessment of recurrence

Contrast-enhanced computed tomography or magnetic resonance imaging was performed every 3 months after surgery. Sites of recurrence were categorised as

Table 1
Prognostic analyses for overall survival and disease-free survival in patients with invasive ductal carcinoma of the pancreas ($n = 170$).

Parameter	n	%	Overall survival			Disease-free survival		
			HR	95% CI	P	HR	95% CI	P
(a) Univariate analysis								
Age ⩾ 65	80	47.1	1.077	0.775–1.498	0.657	1.114	0.808–1.535	0.510
Sex, male	107	62.9	0.876	0.625–1.227	0.442	0.960	0.689–1.339	0.811
ECOG PS ⩾ 1	28	16.5	1.975	1.266–3.081	0.003*	1.403	0.909–2.166	0.126
Absence of adjuvant chemotherapy	110	64.7	1.715	1.186–2.481	0.004*	1.501	1.061–2.123	0.022*
CEA ⩾ 3.4 ng/ml	88	51.8	1.419	1.019–1.975	0.038*	1.584	1.147–2.186	0.005*
CA19-9 ⩾ 111.5 U/ml	85	50.0	0.904	0.648–1.260	0.550	1.026	0.743–1.417	0.877
Tumour differentiation, moderate/poor	126	74.1	1.248	0.857–1.817	0.248	1.514	1.042–2.199	0.030*
Tumour size ⩾ 3.0 cm	81	47.6	1.615	1.160–2.248	0.005*	1.596	1.156–2.203	0.004*
Serosal invasion (+)	46	27.1	0.865	0.591–1.266	0.457	1.164	0.811–1.671	0.411
Retroperitoneal invasion (+)	145	85.3	1.174	0.724–1.904	0.516	1.060	0.668–1.682	0.805
Portal vein invasion (+)	40	23.5	1.479	1.014–2.156	0.042*	1.186	0.818–1.722	0.368
Ly, moderate to severe	46	27.1	1.634	1.130–2.365	0.009*	1.620	1.135–2.312	0.008*
V, moderate to severe	103	60.6	1.779	1.254–2.524	0.001*	1.636	1.168–2.292	0.004*
Ne, moderate to severe	106	62.4	1.812	1.270–2.583	0.001*	1.637	1.164–2.302	0.005*
Lymph node involvement (+)	141	82.9	1.505	0.968–2.341	0.069	1.554	1.002–2.409	0.049*
Pathological stage IIB/III/IV	143	84.1	1.414	0.903–2.214	0.130	1.463	0.937–2.284	0.094
Peripheral CD204%^{high}	85	50.0	1.777	1.272–2.484	0.001*	1.570	1.135–2.172	0.006*
Plx-inv (+)	91	53.5	1.612	1.147–2.264	0.006*	1.785	1.280–2.489	0.001*
Plx-inv distance ⩾ 2500 μm	56	32.9	1.949	1.368–2.777	<0.001*	2.274	1.597–3.238	<0.001*
Plx-inv CD204%^{high}	48	28.2	1.779	1.247–2.539	0.001*	1.904	1.341–2.705	<0.001*
(b) Multivariate analysis								
Absence of adjuvant chemotherapy	110	64.7	1.741	1.143–2.651	0.010*	1.559	1.042–2.332	0.031*
CEA ⩾ 3.4 ng/ml	88	51.8	1.437	1.011–2.041	0.043*	1.602	1.139–2.253	0.007*
Tumour size ⩾ 3.0 cm	81	47.6	1.610	1.147–2.262	0.006*	1.616	1.160–2.250	0.005*
Ly, moderate to severe	46	27.1	1.254	0.839–1.876	0.270	1.151	0.775–1.709	0.487
V, moderate to severe	103	60.6	1.505	1.010–2.242	0.045*	1.291	0.879–1.897	0.192
Peripheral CD204%^{high}	85	50.0	2.167	1.522–3.086	<0.001*	1.831	1.297–2.583	0.001*
Plx-inv CD204%^{high}	48	28.2	2.008	1.362–2.962	<0.001*	2.046	1.400–2.991	<0.001*

* $P < 0.05$. Prognostic analyses were carried out using Cox regression model. HR, hazard ratio; 95% CI, 95% confidence interval; ECOG PS, Eastern Cooperative Oncology Group performance status; CEA, carcinoembryonic antigen; CA19-9, carbohydrate antigen 19-9; Ly, lymphatic invasion; V, vessel invasion; Ne, intrapancreatic neural invasion, Peripheral CD204%^{high}, percentage of CD204-positive cells area at the periphery ⩾ 3.34; Plx-inv, extrapancreatic nerve plexus invasion; Plx-inv CD204%^{high}, percentage of CD204-positive cells area at plx-inv ⩾ 0.57.

liver metastasis, peritoneal dissemination, locoregional recurrence and distant lymph node metastasis. Peritoneal dissemination was defined as marked peritoneal nodules, increased ascites or malignant ascites as confirmed by cytology. Locoregional recurrence was defined as tumour in a dissected space or metastasis in regional lymph nodes according to the 7th edition of the UICC classification [26]. Distant lymph node metastasis was defined as marked lymph node swelling apart from the regional space.

2.6. Statistical analysis

Uni- and multivariate analyses for OS, DFS and time to each type of recurrence were performed using a Cox regression model. Factors showing values of $P < 0.05$ for both OS and DFS in univariate analyses were included in multivariate analyses. Pearson's correlation coefficient r was used to evaluate the correlation among covariates. The observation period was until March 2013, and the median duration was 17.6 months [95% confidence interval (CI), 14.5–20.6]. OS was defined as the time from surgery to death or the date censored at last follow-up. DFS was calculated as the time from surgery to tumour relapse or death or the date censored at last follow-up. Survival curves were drawn using the Kaplan–Meier method, and the differences between patient groups were analysed by log-rank test. P-values were two-sided, with the significance level at $P < 0.05$. Statistical analyses were performed using SPSS version 19.0 software (SPSS, Chicago, IL).

3. Results

3.1. Distribution of CD204%

CD204 accumulation at the primary tumour was measured in all 170 patients, and median CD204% at the tumour periphery was 3.34% [range, 0.16–14.04%]. Plx-inv was observed in 91 patients (53.5%). CD204-positive cells and the measured area at plx-inv are shown in Fig. 1a and b, and CD204-positive cells and the measured area at the tumour periphery are shown in Fig. 1c and d. Median CD204% at plx-inv was 0.57% [range,

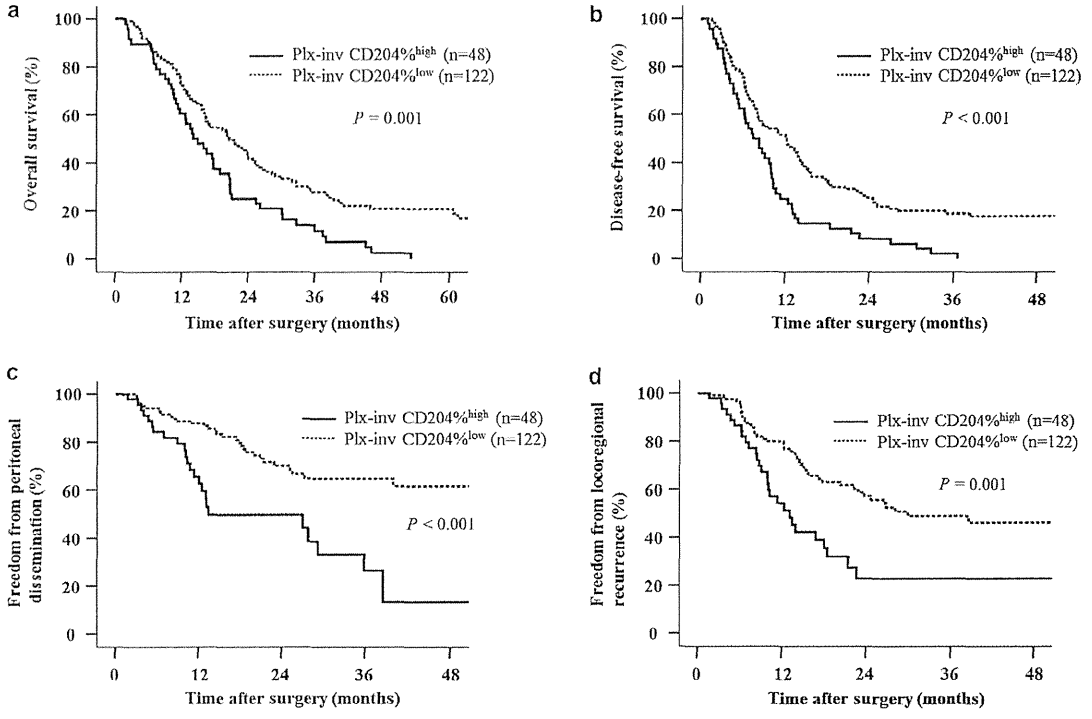

Fig. 2. (a) Kaplan–Meier curve for overall survival stratified by the level of CD204-positive cell area as a percentage at extrapancreatic nerve plexus invasion (plx-inv CD204%). (b) Kaplan–Meier curve for disease-free survival stratified by the level of CD204-positive cell area as a percentage at extrapancreatic nerve plexus invasion (plx-inv CD204%). (c) Kaplan–Meier curve for peritoneal dissemination-free survival stratified by the level of CD204-positive cell area as a percentage at extrapancreatic nerve plexus invasion (plx-inv CD204%). (d) Kaplan–Meier curve for locoregional recurrence-free survival stratified by the level of CD204-positive cell area as a percentage at extrapancreatic nerve plexus invasion (plx-inv CD204%).

0.00–7.76%]. Forty-eight patients with CD204% at plx-inv $\geqslant$0.57% were categorised as plx-inv CD204%^{high}. There were 43 patients with CD204% at plx-inv <0.57% and 79 patients without plx-inv, who were categorised as plx-inv CD204%^{low}.

3.2. Prognostic analyses of clinicopathological factors

The median OS and DFS were 17.8 months [95% CI, 14.7–20.9] and 9.8 months [95% CI, 7.9–11.6], respectively. Univariate analysis identified absence of adjuvant chemotherapy, CEA $\geqslant$ 3.4 ng/ml, tumour size $\geqslant$ 3.0 cm, moderate to severe ly, v and ne, peripheral CD204%^{high}, plx-inv, plx-inv distance $\geqslant$ 2500 μm and plx-inv CD204%^{high} as candidates for correlation with both shorter OS and shorter DFS ($P < 0.05$) (Table 1a). Strong correlations were observed between plx-inv CD204%^{high} and the following covariates: moderate to severe ne, $r = 0.299$, $P < 0.001$; plx-inv, $r = 0.584$, $P < 0.001$; and plx-inv distance $\geqslant$ 2500 μm, $r = 0.534$, $P < 0.001$. Therefore, these covariates were excluded from the multivariate analysis. Multivariate analysis revealed absence of adjuvant chemotherapy (hazard ratio [HR], 1.741; $P = 0.010$), CEA $\geqslant$ 3.4 ng/ml (HR, 1.437; $P = 0.043$), tumour size $\geqslant$ 3.0 cm (HR, 1.610; $P = 0.006$), moderate to severe v (HR, 1.505; $P = 0.045$), peripheral CD204%^{high} (HR, 2.167; $P < 0.001$), and plx-inv CD204%^{high} (HR, 2.008; $P < 0.001$) as independent risk factors for shorter OS (Table 1b). In terms of DFS, absence of adjuvant chemotherapy (HR, 1.559; $P = 0.031$), CEA $\geqslant$ 3.4 ng/ml (HR, 1.602; $P = 0.007$), tumour size $\geqslant$ 3.0 cm (HR, 1.616; $P = 0.005$), peripheral CD204%^{high} (HR, 1.831; $P = 0.001$) and plx-inv CD204%^{high} (HR, 2.046; $P < 0.001$) represented independent risk factors for shorter DFS (Table 1b). OS and DFS curves according to the level of plx-inv CD204% are shown in Fig. 2a and b.

3.3. Time to relapse according to site of recurrence

Median times to tumour relapse were 7.3 months [95% CI, 5.5–9.1] for liver metastasis (71 patients, 41.8%), 12.1 months [9.2–15.0] for peritoneal dissemination (57 patients, 33.5%), 10.0 months [7.1–13.0] for locoregional recurrence (76 patients, 44.7%) and 8.8 months [4.0–13.6] for distant lymph node recurrence (46 patients, 27.1%). Multivariate analyses showed that absence of adjuvant chemotherapy (HR, 1.924; $P = 0.030$) and moderate to severe ly (HR, 2.634; $P < 0.001$) correlated with early relapse to liver metastasis (Table 2). Peripheral CD204%^{high} was a predictor of peritoneal dissemination (HR, 1.815; $P = 0.031$)

(Table 2). Plx-inv CD204%^{high} was independently associated with peritoneal dissemination (HR, 2.886; $P < 0.001$) and locoregional recurrence (HR, 2.483; $P < 0.001$) (Table 2 and Fig. 2c and d).

3.4. Prognostic analyses stratified by presence of adjuvant chemotherapy

Adjuvant chemotherapy represented an independent prognostic factor for OS and DFS as a definitive therapeutic modality (Table 1, Fig. 3a and b). Multivariate analyses to test prognostic factors with adjuvant chemotherapy were re-examined and revealed that only plx-inv CD204%^{high} was associated with both shorter OS (HR, 2.624; $P = 0.011$) and shorter DFS (HR, 2.257; $P = 0.038$) in patients with plx-inv who underwent postoperative adjuvant chemotherapy (Table 3).

4. Discussion

The present study demonstrated that the accumulation of CD204-positive cells, representing M2 macrophages, at plx-inv of pancreatic IDC was an independent predictor of shorter OS and DFS in patients who underwent curative pancreaticoduodenectomy for pancreatic IDC. The prognostic impact of plx-inv CD204%^{high} was maintained in patients who received adjuvant chemotherapy. Infiltration of M2 macrophages at plx-inv of pancreatic IDC was revealed as a key factor to explain the aggressiveness of pancreatic IDC for the first time in this study.

Peritoneal dissemination has long been considered a poor prognostic factor for patients with pancreatic IDC [27–29]. Patients with plx-inv CD204%^{high} showed early relapse to the peritoneal cavity in this study. The interaction between M2 macrophages and tumour cells at plx-inv was suggested to play a crucial role in peritoneal recurrence, which led to poor survival. From the perspective of surgical anatomy, nerve fibres of the plexus pancreaticus capitalis might provide a convenient pathway for infiltrating tumour cells. As recent experimental study showed that macrophages around nerves were recruited in response to cytokine secreted by invading tumour cells and increased migration of tumour cells [15], M2 macrophages might promote the invasiveness of tumour cells at plx-inv, leading tumour cells to disperse into the peritoneal space and resulting in peritoneal dissemination. This speculation warrants further studies to observe the distribution of M2 macrophages in metastatic sites of pancreatic IDC and to test the role of M2 macrophages in metastatic tumour models.

Immunophysiologically, neural injury leads to the accumulation of macrophages in the peripheral nerve system, although few macrophages exist in intact nerves [30]. Ceyhan et al. reported that neuritis was caused by the invasion of malignant tumour cells into the pancreas

Table 2
Multivariate analysis for early relapse according to the sites of recurrence in patients with invasive ductal carcinoma of the pancreas ($n = 170$).

Parameter	Liver metastasis ($n = 71$)				Peritoneal dissemination ($n = 57$)				Locoregional recurrence ($n = 76$)				Distant lymph node metastasis (n = 46)			
	n	%	HR	95% CI	*P*	*n*	%	HR	95% CI	*P*	*n*	%	HR	95% CI	*P*	*n*	%	HR	95% CI	*P*
Absence of adjuvant chemotherapy	50	70.4	1.924	1.065–3.476	0.030*	34	59.6	1.107	0.602–2.036	0.743	52	68.4	1.734	0.995–3.022	0.052	32	69.6	1.660	0.794–3.471	0.178
CEA ⩾ 3.4 ng/ml	40	56.3	1.347	0.819–2.215	0.241	23	40.4	0.934	0.531–1.640	0.811	36	47.4	1.238	0.773–1.985	0.374	26	56.5	1.516	0.810–2.839	0.193
Tumour size ⩾ 3.0 cm	38	53.5	1.492	0.925–2.405	0.101	22	38.6	0.968	0.558–1.681	0.909	34	44.7	1.114	0.698–1.780	0.650	23	50.0	1.327	0.732–2.407	0.351
Ly, moderate to severe	28	39.4	2.634	1.574–4.408	<0.001*	14	24.6	0.839	0.436–1.617	0.601	21	27.6	0.878	0.501–1.539	0.649	17	37.0	1.909	0.993–3.671	0.053
V, moderate to severe	46	64.8	1.146	0.660–1.988	0.629	30	52.6	1.126	0.618–2.052	0.698	47	61.8	1.323	0.774–2.261	0.306	29	63.0	1.133	0.560–2.292	0.729
Peripheral CD204%^{high}	37	52.1	1.517	0.931–2.472	0.095	30	52.6	1.815	1.055–3.124	0.031*	36	47.4	1.501	0.933–2.417	0.094	21	45.7	1.305	0.706–2.412	0.396
Plx-inv CD204%^{high}	18	25.4	0.916	0.518–1.619	0.763	24	42.1	2.886	1.615–5.159	<0.001*	28	36.8	2.483	1.485–4.151	<0.001*	15	32.6	1.564	0.795–3.073	0.195

* $P < 0.05$. Multivariate analysis was carried out using Cox regression hazard model. HR, hazard ratio; 95% CI, 95% confidence interval; CEA, carcinoembryonic antigen; Ly, lymphatic invasion; V, vessel invasion; Peripheral CD204%^{high}, percentage of CD204-positive cells area at the periphery ⩾ 3.34; Plx-inv CD204%^{high}, percentage of CD204-positive cells area at extrapancreatic nerve plexus invasion ⩾ 0.57.

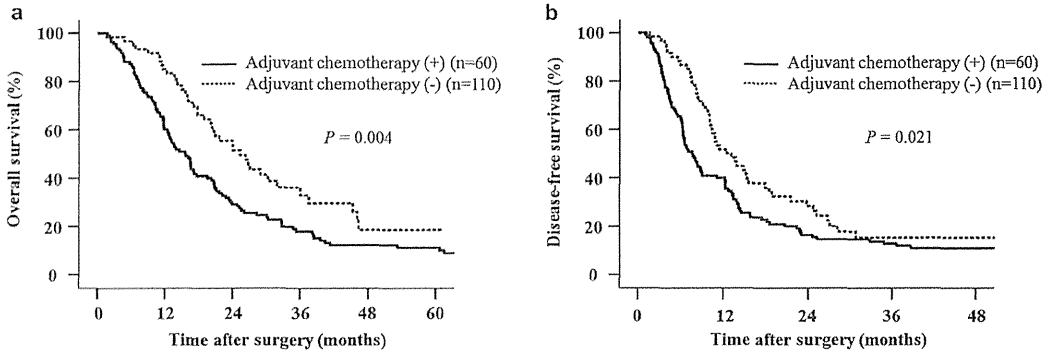

Fig. 3. (a) Kaplan–Meier curve for overall survival stratified by the presence of adjuvant chemotherapy. (b) Kaplan–Meier curve for disease-free survival stratified by the presence of adjuvant chemotherapy.

Table 3
Multivariate analysis for overall survival and disease-free survival in patients who received adjuvant chemotherapy ($n = 60$).

Parameter	n	%	Overall survival			Disease-free survival		
			HR	95% CI	P	HR	95% CI	P
CEA $\geqslant$ 3.4 ng/ml	23	38.3	1.514	0.704–3.257	0.289	1.883	0.969–3.658	0.062
Tumour size $\geqslant$ 3.0 cm	26	43.3	1.283	0.663–2.484	0.460	1.179	0.641–2.170	0.596
Ly, moderate to severe	21	35.0	1.775	0.833–3.782	0.137	1.475	0.667–3.263	0.337
V, moderate to severe	19	31.7	2.178	1.059–4.479	0.034*	1.476	0.769–2.833	0.242
Peripheral CD204%^{high}	32	53.3	1.206	0.601–2.420	0.598	0.890	0.472–1.679	0.719
Plx-inv CD204%^{high}	20	33.3	2.624	1.242–5.544	0.011*	2.257	1.045–4.879	0.038*

* $P < 0.05$. Multivariate analysis was carried out using Cox regression model. HR, hazard ratio; 95% CI, 95% confidence interval; CEA, carcinoembryonic antigen; Ly, lymphatic invasion; V, vessel invasion; Peripheral CD204%^{high}, percentage of CD204-positive cells area at the periphery $\geqslant$ 3.34; Plx-inv CD204%^{high}, percentage of CD204-positive cells area at extrapancreatic nerve plexus invasion $\geqslant$ 0.57.

[31]. In our previous experimental study [12], neural invasion over a long distance could lead to severe neural damage. Additionally, the present study showed strong positive correlations among ne, plx-inv, long plx-inv distance and plx-inv CD204%^{high}. Taken together with the paracrine regulation between macrophages and tumour cells at plx-inv [14,15], severe neural invasion of tumour cells appears to recruit M2 macrophages due to neural damage. Moreover, the neural system was suggested as an expedient structure for interaction between tumour cells and M2 macrophages that promotes pancreatic cancer cell proliferation.

Adjuvant chemotherapy after complete resection of pancreatic IDC has been established as the definitive standard of care within the last decade [24,32,33]. In the present study, plx-inv CD204%^{high} was the only independent prognostic factor for poor OS and DFS in the group of patients with adjuvant chemotherapy. According to recent reports, immunoregulatory cytokines such as interleukin-6 and prostaglandin E2, which are present in the tumour microenvironment, are associated with chemoresistance and tumour-induced differentiation of tumour-promoting M2 macrophages [34,35]. Additional therapy to suppress M2 macrophages might thus prove effective, particularly against cases with plx-inv and high accumulation of M2 macrophages. Depletion of macrophages by zoledronic acid has been reported to enhance the effects of sorafenib in an *in vivo* model of metastatic liver cancer [36]. A phase II randomised controlled study of tasquinimod (oral quinolone-3-carboxamide) for metastatic castrate-resistant prostate cancer patients prolonged progression-free survival and confirmed the pharmacological efficacy of this agent for inhibiting S100A9 [37], which is a protein expressed in inflammatory cells that induces the maturation of macrophages [38]. Therefore, anti-M2 macrophage therapy may have potential as an innovative treatment for pancreatic IDC.

Limitations of this study include the retrospective manner of the investigation. Adjuvant chemotherapy was performed in 60 patients and was an independent factor predictive of OS and DFS, but the indication was influenced by time trends, and some degree of selection bias might have been present. Although OS and DFS for our patient cohort were comparable with the other previous studies [24,32,33], further investigation in patients with standardised adjuvant chemotherapy is needed. Moreover, since only resectable pancreatic cancer was studied, it is unknown whether the results can be extrapolated to the much higher numbers of unresectable cases.

In conclusion, pancreatic cancer patients with high accumulation of CD204-positive cells at plx-inv who underwent curative resection showed a high incidence

of recurrence in the form of peritoneal dissemination and locoregional recurrence and shorter OS and DFS. The impact of CD204-positive cells at plx-inv on OS and DFS was maintained in the setting of adjuvant chemotherapy. Increased infiltration of M2 macrophages at plx-inv may represent an important finding for detecting patients with aggressive IDC of the pancreas.

Conflict of interest statement

None declared.

Acknowledgement

Supported by Grants-In-Aid for Cancer Research and for the Third-term Comprehensive 10-year Strategy for Cancer Control from the Ministry of Health, Labour and Welfare of Japan; JSPS KAKENHI Grant Number 22790624; the National Cancer Center Research and Development Fund (23-A-2b).

References

[1] Siegel R, Ward E, Brawley O, et al. Cancer statistics, 2011: the impact of eliminating socioeconomic and racial disparities on premature cancer deaths. CA Cancer J Clin 2011;61:212–36.
[2] Hernandez JM, Morton CA, Al-Saadi S, et al. The natural history of resected pancreatic cancer without adjuvant chemotherapy. Am Surg 2010;76:480–5.
[3] Mitsunaga S, Hasebe T, Kinoshita T, et al. Detail histologic analysis of nerve plexus invasion in invasive ductal carcinoma of the pancreas and its prognostic impact. Am J Surg Pathol 2007;31:1636–44.
[4] Nagakawa T, Mori K, Nakano T, et al. Perineural invasion of carcinoma of the pancreas and biliary tract. Br J Surg 1993;80:619–21.
[5] Nakao A, Harada A, Nonami T, et al. Clinical significance of carcinoma invasion of the extrapancreatic nerve plexus in pancreatic cancer. Pancreas 1996;12:357–61.
[6] Chatterjee D, Katz MH, Rashid A, et al. Perineural and intraneural invasion in posttherapy pancreaticoduodenectomy specimens predicts poor prognosis in patients with pancreatic ductal adenocarcinoma. Am J Surg Pathol 2012;36:409–17.
[7] Takahashi H, Ohigashi H, Ishikawa O, et al. Perineural invasion and lymph node involvement as indicators of surgical outcome and pattern of recurrence in the setting of preoperative gemcitabine-based chemoradiation therapy for resectable pancreatic cancer. Ann Surg 2012;255:95–102.
[8] Tempero MA, Arnoletti JP, Behrman SW, et al. National Comprehensive Cancer Networks. Pancreatic Adenocarcinoma, version 2.2012: featured updates to the NCCN Guidelines. J Natl Compr Cancer Networks 2012;10:703–13.
[9] Imoto A, Mitsunaga S, Inagaki M, et al. Neural invasion induces cachexia via astrocytic activation of neural route in pancreatic cancer. Int J Cancer 2012;131:2795–807.
[10] Takahashi S, Hasebe T, Oda T, et al. Extra-tumor perineural invasion predicts postoperative development of peritoneal dissemination in pancreatic ductal adenocarcinoma. Anticancer Res 2001;21:1407–12.
[11] Zhu Z, Friess H, diMola FF, et al. Nerve growth factor expression correlates with perineural invasion and pain in human pancreatic cancer. J Clin Oncol 1999;17:2419–28.
[12] Mitsunaga S, Fujii S, Ishii G, et al. Nerve invasion distance is dependent on laminin gamma2 in tumors of pancreatic cancer. Int J Cancer 2010;127:805–19.
[13] Dai H, Li R, Wheeler T, et al. Enhanced survival in perineural invasion of pancreatic cancer: an in vitro approach. Hum Pathol 2007;38:299–307.
[14] Gil Z, Cavel O, Kelly K, et al. Paracrine regulation of pancreatic cancer cell invasion by peripheral nerves. J Natl Cancer Inst 2010;102:107–18.
[15] Cavel O, Shomron O, Shabtay A, et al. Endoneurial macrophages induce perineural invasion of pancreatic cancer cells by secretion of GDNF and activation of RET tyrosine kinase receptor. Cancer Res 2012;72:5733–43.
[16] Spilsbury K, O'Mara MA, Wu WM, et al. Isolation of a novel macrophage-specific gene by differential cDNA analysis. Blood 1995;85:1620–9.
[17] Ripoll VM, Irvine KM, Ravasi T, et al. Gpnmb is induced in macrophages by IFN-gamma and lipopolysaccharide and acts as a feedback regulator of proinflammatory responses. J Immunol 2007;178:6557–66.
[18] Mantovani A, Sozzani S, Locati M, et al. Macrophage polarization: tumor-associated macrophages as a paradigm for polarized M2 mononuclear phagocytes. Trends Immunol 2002;23:549–55.
[19] Ryder M, Ghossein RA, Ricarte-Filho JC, et al. Increased density of tumor-associated macrophages is associated with decreased survival in advanced thyroid cancer. Endocr Relat Cancer 2008;15:1069–74.
[20] Lissbrant IF, Stattin P, Wikstrom P, et al. Tumor associated macrophages in human prostate cancer: relation to clinicopathological variables and survival. Int J Oncol 2000;17:445–51.
[21] Ma YY, He XJ, Wang HJ, et al. Interaction of coagulation factors and tumor-associated macrophages mediates migration and invasion of gastric cancer. Cancer Sci 2011;102:336–42.
[22] Subimerb C, Pinlaor S, Khuntikeo N, et al. Tissue invasive macrophage density is correlated with prognosis in cholangiocarcinoma. Mol Med Report 2010;3:597–605.
[23] Yoshikawa K, Mitsunaga S, Kinoshita T, et al. Impact of tumor-associated macrophages on invasive ductal carcinoma of the pancreas head. Cancer Sci 2012;103:2012–20.
[24] Ueno H, Kosuge T, Matsuyama Y, et al. A randomised phase III trial comparing gemcitabine with surgery-only in patients with resected pancreatic cancer: Japanese Study Group of Adjuvant Therapy for Pancreatic Cancer. Br J Cancer 2009;101:908–15.
[25] Japan Pancreas Society. Classification of pancreatic carcinoma. 6th ed. Tokyo: Kanehara; 2009.
[26] Sobin LH, Gospodarowicz MK, Wittekind C. International union against cancer: TNM classification of malignant tumours. 7th ed. New York: Wiley-Blackwell; 2009.
[27] Fujino Y, Suzuki Y, Ajiki T, et al. Predicting factors for survival of patients with unresectable pancreatic cancer: a management guideline. Hepatogastroenterology 2003;50:250–3.
[28] Nakachi K, Furuse J, Ishii H, et al. Prognostic factors in patients with gemcitabine-refractory pancreatic cancer. Jpn J Clin Oncol 2007;37:114–20.
[29] Morizane C, Okusaka T, Morita S, et al. Construction and validation of a prognostic index for patients with metastatic pancreatic adenocarcinoma. Pancreas 2011;40:415–21.
[30] Rotshenker S. Wallerian degeneration: the innate-immune response to traumatic nerve injury. J Neuroinflammation 2011;8:109.
[31] Ceyhan GO, Bergmann F, Kadihasanoglu M, et al. Pancreatic neuropathy and neuropathic pain–a comprehensive pathomorphological study of 546 cases. Gastroenterology 2009;136:177–86.
[32] Neoptolemos JP, Stocken DD, Friess H, et al. A randomized trial of chemoradiotherapy and chemotherapy after resection of pancreatic cancer. N Engl J Med 2004;350:1200–10.
[33] Oettle H, Post S, Neuhaus P, et al. Adjuvant chemotherapy with gemcitabine vs observation in patients undergoing curative-intent

resection of pancreatic cancer: a randomized controlled trial. JAMA 2007;297:267–77.

[34] Dijkgraaf EM, Heusinkveld M, Tummers B, et al. Chemotherapy alters monocyte differentiation to favor generation of cancer-supporting M2 macrophages in the tumor microenvironment. Cancer Res 2013;73:2480–92.

[35] Zitvogel L, Apetoh L, Ghiringhelli F, Kroemer G. Immunological aspects of cancer chemotherapy. Nat Rev Immunol 2008; 8(1):59–73.

[36] Zhang W, Zhu XD, Sun HC, et al. Depletion of tumor-associated macrophages enhances the effect of sorafenib in metastatic liver cancer models by antimetastatic and antiangiogenic effects. Clin Cancer Res 2010;16:3420–30.

[37] Pili R, Häggman M, Stadler WM, et al. Phase II randomized, double-blind, placebo-controlled study of tasquinimod in men with minimally symptomatic metastatic castrate-resistant prostate cancer. J Clin Oncol 2011;29:4022–8.

[38] Sinha P, Okoro C, Foell D, et al. Proinflammatory S100 proteins regulate the accumulation of myeloid-derived suppressor cells. J Immunol 2008;181:4666–75.

What is the nature of pancreatic consistency? Assessment of the elastic modulus of the pancreas and comparison with tactile sensation, histology, and occurrence of postoperative pancreatic fistula after pancreaticoduodenectomy

Motokazu Sugimoto, MD, PhD,[a,b] Shinichiro Takahashi, MD, PhD,[a] Motohiro Kojima, MD, PhD,[b] Naoto Gotohda, MD, PhD,[a] Yuichiro Kato, MD,[a] Shingo Kawano, MD,[b] Atsushi Ochiai, MD, PhD,[b] *and* **Masaru Konishi, MD,[a]** *Chiba, Japan*

Background. *Although pancreatic consistency is a factor known to have an impact on the occurrence of postoperative pancreatic fistula (POPF) after pancreaticoduodenectomy (PD), it usually is assessed subjectively by the surgeon. Measurement of the elastic modulus (EM), a parameter characterizing the elasticity of a material, may be one approach for achieving objective and quantitative assessment of pancreatic consistency. This study was conducted to investigate the utility of determining the EM of the pancreas.*

Methods. *Fifty-nine patients who underwent PD and measurement of the EM of the ex vivo pancreas were investigated. Data for EM were compared with the tactile evaluation made by surgeons, histologic findings, and the occurrence of POPF.*

Results. *The EM of the pancreas was correlated with the tactile evaluation made by the surgeon (soft pancreas, 1.4 ± 2.1 kPa vs hard pancreas, 4.4 ± 5.1 kPa; P < .001). An EM of > 3.0 kPa was correlated with histologic findings including increased ratios of azan-Mallory positivity (P = .003) and α-smooth muscle actin positivity (P = .006), a decreased lobular ratio (P = .021), and an increased vessel density (P < .001). Patients with a pancreatic EM of < 3.0 kPa had an increased risk of POPF (hazard ratio, 9.333; P = .002).*

Conclusion. *Assessment of the EM of the resected pancreas reflects the tactile evaluation made by the surgeon and histological degree of pancreatic fibrosis, and is correlated with the occurrence of POPF after PD. (Surgery 2014;156:1204-11.)*

From the Department of Hepatobiliary-Pancreatic Surgery[a] and Division of Pathology,[b] Research Center for Innovative Oncology, National Cancer Center Hospital East, Kashiwa, Chiba, Japan

THE CONSISTENCY OF THE PANCREAS is a factor known to have an impact on the occurrence of postoperative pancreatic fistula (POPF) after pancreatic resection. In relation to pancreaticoduodenectomy (PD), it is accepted among pancreatic surgeons that in comparison with a "hard" pancreatic consistency, a "soft" consistency is associated with a greater incidence of POPF.[1-5] Pancreatic consistency usually is evaluated intraoperatively on the basis of the tactile sensation felt by surgeons and is thus a subjective and qualitative assessment.

The elastic modulus (EM) is a physical parameter[6] that characterizes the elasticity of a material. It

Supported in part by Health and Labour Sciences Research Grants for the Third Term Comprehensive Control Research for Cancer from the Ministry of Health, Labour and Welfare of Japan.

Accepted for publication May 16, 2014.

Reprint requests: Shinichiro Takahashi, MD, PhD, National Cancer Center Hospital East, 6-5-1 Kashiwa-no-ha, Kashiwa, Chiba 277-8577, Japan. E-mail: shtakaha@east.ncc.go.jp.

0039-6060/$ - see front matter

© 2014 Elsevier Inc. All rights reserved.

http://dx.doi.org/10.1016/j.surg.2014.05.015

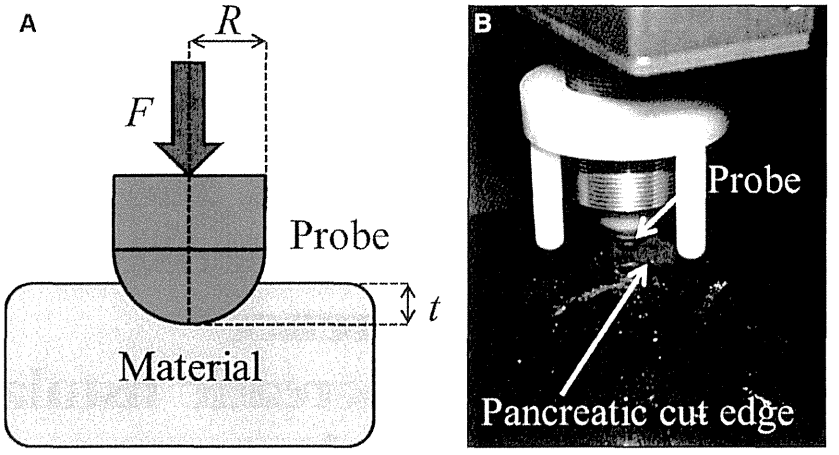

Fig 1. (*A*) Elastic material is indented vertically by a rigid spherical indenter probe. The elastic modulus (EM) of the material is calculated based on the contact stress theory of Hertz. *F*, Force exerted on an object under tension; *t*, variant of compression; *R*, radius of the spherical indenter probe. (*B*) Pancreatic cut surface (shown in *orange*) was indented vertically by a rigid spherical probe and released at a constant computer-controlled velocity. EM of the pancreas at an arbitrary indentation depth was calculated automatically. This procedure was performed using a Venustron apparatus.

has been applied for direct measurement of the elasticity of human tissues such as skin, bone, breast, and brain.[7-13] Different organs have a wide range of elasticity, and the elasticity of a specific organ may be altered as a result of various disease processes. For instance, Samani et al[12] reported that the mean EM of normal breast tissue was 1.9 kPa, that of fibroadenoma was 11.42 kPa, and that of invasive ductal carcinoma was 22.55 kPa.

With recent advances in diagnostic radiology, ultrasound elastography of the pancreas via the use of a transcutaneous or endoscopic approach has been reported increasingly for differential diagnosis of focal pancreatic lesions and pancreatic fibrosis.[14-19] Analyses that use endoscopic ultrasound elastography have demonstrated that the elastic parameters of the pancreatic parenchyma calculated by setting the surrounding soft tissue as a control are correlated with the degree of fibrotic change in the resected specimen.[14] The technique of elastography has now made it possible to evaluate a region of interest both qualitatively and quantitatively by monitoring the localized tissue displacement resulting from short-duration acoustic excitation to derive information on elasticity.[15]

To our knowledge, however, the feasibility of direct measurement of the EM of pancreatic tissue has never been evaluated. Comparison between the EM and the histologic characteristics of the pancreas may allow a better understanding of pathologic alterations of the pancreatic parenchyma, which may affect the consistency of the pancreas. Moreover, objective and quantitative evaluation of the EM of the pancreatic parenchyma might become a more widely acceptable means of assessing the risk of POPF after PD than is the case for subjective and qualitative assessment by the surgeon. The aim of the present study was to investigate the utility of assessment of the EM of the pancreas by evaluating its correlation with tactile sensation, histological findings, and the occurrence of POPF after PD.

METHODS

Patients and clinical data collection. Between November 2011 and May 2013, 59 PD specimens were used for ex vivo measurement of the EM of resected pancreas at the National Cancer Center Hospital East. The cut edge of the resected pancreas was evaluated histopathologically in all specimens to determine whether a sufficient operative margin for exclusion of tumor cells had been secured. Clinicopathologic data were reviewed from the medical records. During this period, the method used for reconstruction of the remnant pancreas and postoperative management were standardized. The study was approved by the institutional review board of the National Cancer Center (2012-067).

Operative techniques and perioperative management. Details of the operative maneuvers and perioperative management were described in our previous paper.[20] To summarize, subtotal stomach-preserving PD with D2 lymphadenectomy and modified Child's reconstruction were performed in all cases. End-to-side pancreaticojejunostomy was performed as a two-layered anastomosis with

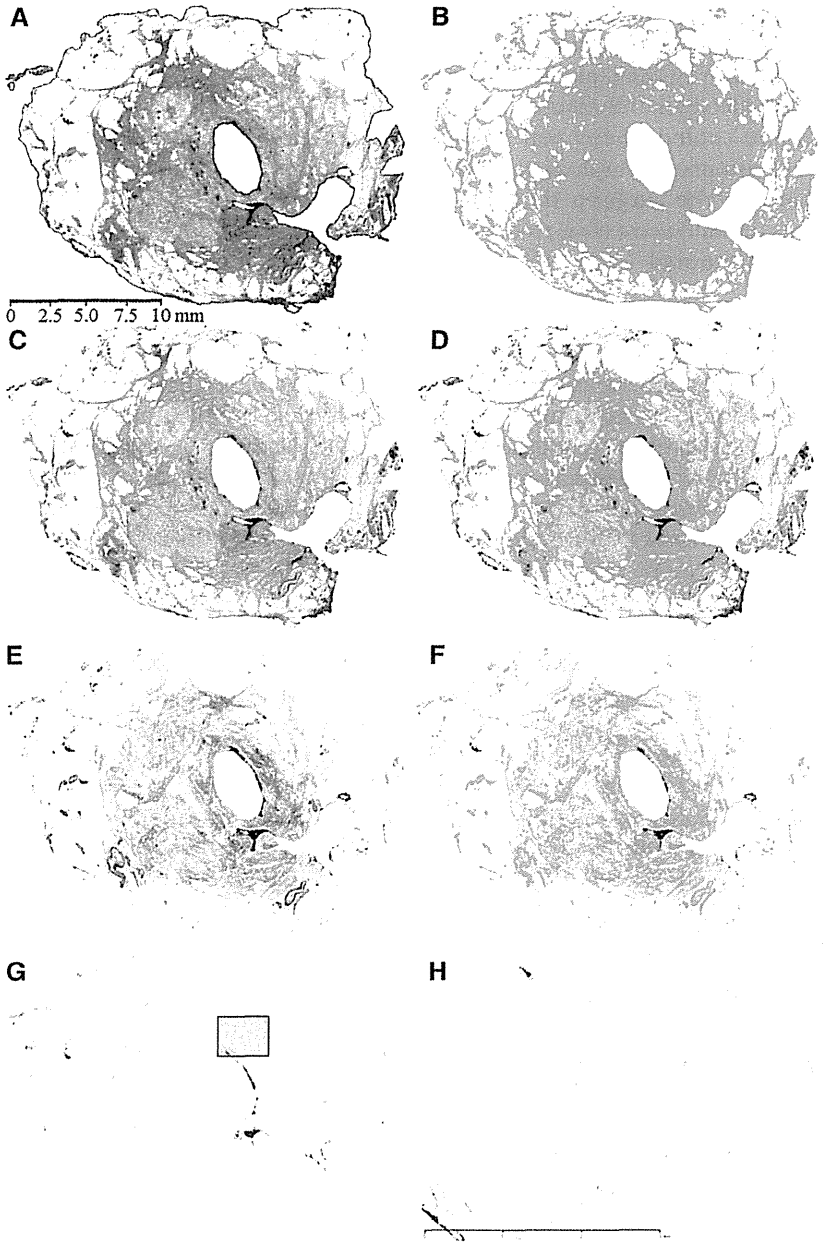

Fig 2. Histologic evaluation of the pancreatic stump. In this case, the EM of the pancreas was 13.0 kPa and the patient did not develop postoperative pancreatic fistula (POPF). (*A*) Loupe image of hematoxylin and eosin (HE)-stained slide. The outer circumference of the entire cut surface (*red line*) and the inner circumference of the main pancreatic duct (MPD) lumen (*blue line*) were automatically outlined, and these areas were calculated using the tracing algorithm of the WinROOF version 6.5 software (Mitani Corporation, Tokyo, Japan). The area of an entire cut surface (within the *red line*) was 367.0 mm^2, and the MPD area (within the *blue line*) was 10.59 mm^2. The MPD ratio was 2.89%, calculated as the percentage area of MPD in the entire cut surface. (*B*) The HE-positive area was determined as the visualized area stained with HE using the color-detecting algorithm of the software and identified as *bright green* in this image. The area of fat was defined as the area of an entire cut surface minus the MPD area and the HE-positive area. The fat ratio was 37.5%, calculated as the percentage area of fat in an entire cut surface. (*C*) Azan-Mallory (azan) staining was evaluated on the loupe image to determine the degree of fibrosis. (*D*) The azan-positive area was determined as the visualized area stained with aniline blue using the color-detecting algorithm of the software, and identified as *bright green* in this image. The azan-positive ratio was 24.8%, calculated as the percentage area of azan positivity in an entire cut surface. The lobular area was defined as the HE-positive area minus the MPD area and the azan-positive area. The lobular ratio was 34.8%, calculated as the percentage area of lobules in an entire cut surface. (*E*) Loupe image of

the use of interrupted duct-to-mucosa sutures and coverage of the entire cut surface of the pancreas with the seromuscular layer of the jejunum. Closed suction drains were placed in the vicinity of the pancreaticojejunal and choledochojejunal anastomosis. Pancreatic consistency was evaluated subjectively as soft or hard by the surgeon during the operation. POPF was defined according to the classification of the International Study Group on Pancreatic Fistula.[21]

Measurement of the EM of the resected pancreas. After the PD specimen had been resected, it was immediately subjected to ex vivo measurement. The EM, also known as Young's modulus, is a measure of the stiffness of an elastic material.[6] It is defined as the ratio of the stress along an axis over the strain along that axis within the range of stress covered by Hooke's law. Stress is the degree of compressive loading and strain is the amount of deformation, both of which are generated by external force imposed on a material. The EM can be derived experimentally from a stress-strain curve generated by conducting tensile testing of a material sample.

In a model for which Hooke's law holds, the EM is a characteristic of an elastic material determined from the distortion resulting from loading and the recovery observed upon unloading. According to the contact stress theory of Hertz,[22,23] when an elastic material is compressed vertically by a rigid spherical probe, the EM (E) of the material is defined by the following formula, based on the relationships among force (F), Poisson's ratio (ν), a variant of compression (t), and the radius (R) of the rigid spherical probe compressing the material vertically (Fig 1, *A*).

$$E = \frac{3}{4} \cdot F \cdot \left(1 - v^2\right) \cdot t^{-\frac{3}{2}} \cdot R^{-\frac{1}{2}}$$

The EM of the resected pancreas was measured using a Venustron (Axiom, Koriyama, Japan) automatic indentation apparatus[24] (Fig 1, *B*), based on Hooke's law and Hertz's contact stress theory.[6,22,23] The whole specimen was placed on a board with sufficient stability, and the pancreatic cut edge was directed just upward so that the probe could be directed vertically toward the organ surface. A rigid spherical probe with a radius (R) of 2.5 mm indented the pancreatic cut edge vertically for 4.0 mm after making contact with the surface, and then released, at a computer-controlled constant velocity (1.5 mm/s). The initial contact pressure was set at 1.0 gf/mm^2 by a built-in motor. The EM of the specimen was calculated for every 0.005 mm of indentation depth, and the EM at a loading depth of 1.25 mm was used for the analysis. Poisson's ratio was set at 0.49.[7,25,26]

Consecutive measurements of the EM were performed three times at each of three points on the pancreatic cut surface, and the average value of the three median values for each point was then used for the analysis. Before the start of this trial, silicon objects with a tactile sensation similar to that of the human pancreas were used to calibrate the experimental apparatus with appropriate values, and 10 resected pancreatic specimens were tested preliminarily to provide a learning curve for the measurement procedure. In every case, the measurement procedure and circumstances were standardized, and all experiments were performed by a single investigator (M.S.).

Histologic evaluation. Formalin-fixed, paraffin-embedded specimens obtained from a pancreatic stump were cut into 3-μm-thick serial sections. The sections were stained with hematoxylin and eosin (HE) and azan-Mallory (azan) and by immunohistochemistry for α-smooth muscle actin (α-SMA) and CD31. Immunohistochemical staining for α-SMA and CD31 was performed automatically on a Ventana Benchmark ULTRA (Ventana Medical Systems, Tucson, AZ). Monoclonal antihuman α-SMA antibody (Dako, Glostrup, Denmark) was used at a dilution of 1:100, and the conditions for antigen retrieval and primary antibody incubation were set at 91°C for 8 minutes and 35°C for 60 minutes, respectively. Antihuman CD31 antibody (Dako, Glostrup, Denmark) was used at a dilution of 1:200, and antigen retrieval and primary antibody incubation were performed at 95°C for 8 minutes and 35°C for 60 minutes, respectively.

The slides were photographed using a NanoZoomer Digital Pathology Virtual Slide Viewer (Hamamatsu Photonics, Hamamatsu, Japan) and subjected to morphometric analysis. In loupe

immunohistochemical staining for α-smooth muscle actin (α-SMA). (*F*) The α-SMA-positive area was identified as *bright green* using the color-detecting algorithm of the software. The α-SMA-positive ratio was 10.7%, calculated as the percentage area of α-SMA-positive in an entire cut surface. (*G*) Loupe image of immunohistochemical staining for CD31. (*H*) Immunohistochemical staining for CD31 at ×4.0 magnification in the *blue square* shown in (*G*). The number of vessels was counted in terms of the CD31-immunopositive luminal structures visible in each field. The total number of vessels in an entire cut surface was 1,010, and the vessel density was 2.8/mm^2.

images of HE-stained slides, the outer circumference of the entire cut surface and inner circumference of the main pancreatic duct (MPD) lumen were automatically outlined, and their areas were calculated using the tracing algorithm of the WinROOF version 6.5 software (Mitani Corporation, Tokyo, Japan). HE- and azan-positive areas and α-SMA-immunopositive areas were identified and calculated on the loupe image, using each color-detecting algorithm of the software.

The area of fat was defined as the area of an entire cut surface minus the MPD area and HE-positive area, and the lobular area was defined as the HE-positive area minus the azan-positive area. The number of vessels was counted manually as CD31-immunopositive luminal structures detectable at a magnification of ×4.0 in an entire cut surface. The MPD ratio was calculated as MPD area/area of an entire cut surface × 100, the fat ratio as (area of an entire cut surface − MPD area − HE-positive area)/area of an entire cut surface × 100, the azan-positive ratio as azan-positive area/area of an entire cut surface × 100, α-SMA-positive ratio as α-SMA-positive area/area of an entire cut surface × 100, vessel density as number of vessels/area of an entire cut surface × 100, and lobular ratio as (HE-positive area − azan-positive area)/area of an entire cut surface × 100. Histological analyses of a case are shown in Fig 2. One investigator (M.S.) performed all of the histological analyses under the supervision of an experienced pathologist (M.K.).

Statistical analysis. Data for the EM of the resected pancreatic cut surface were compared between patients whose pancreatic consistency palpated intraoperatively was soft and hard, using Mann-Whitney *U* test. Correlation between EM and histological findings was evaluated with Spearman correlation coefficient ρ. Histological data were compared between the cases showing low and high EM by use of the Mann-Whitney *U* test. The Mann-Whitney *U* test also was used to compare the EM between patients who did and did not develop POPF after PD. Logistic regression analysis was used to evaluate the risk of POPF occurrence. Numerical data were expressed as median ± SD. All *P* values were based on two-sided statistical tests, setting the significance level as .05. All statistical analyses were performed using the SPSS Statistics version 19.0 software (SPSS, Chicago, IL).

RESULTS

Correlation between EM and tactile sensation of the pancreas. The median EM of the pancreatic cut edge for 59 cases was 2.0 ± 4.3 kPa. The pancreas was palpated as soft for 31 patients and as hard for 28 patients. The EM of the pancreas in cases that were judged as soft and hard was 1.4 ± 2.1 kPa and 4.4 ± 5.1 kPa, respectively ($P < .001$) (Fig 3). Because the EM was strongly correlated with the tactile sensation felt by surgeons, the EM cut-off value was determined using the receiver operating characteristic curve for its relationship with the tactile sensation. The area under the receiver operating characteristic curve for the correlation between the EM and tactile sensation of the pancreas was 0.862. When 3.0 kPa was set as the cut-off value for the EM, sensitivity, specificity, positive predictive value, and negative predictive value were 75.0%, 90.3%, 87.5%, and 80.0%, respectively.

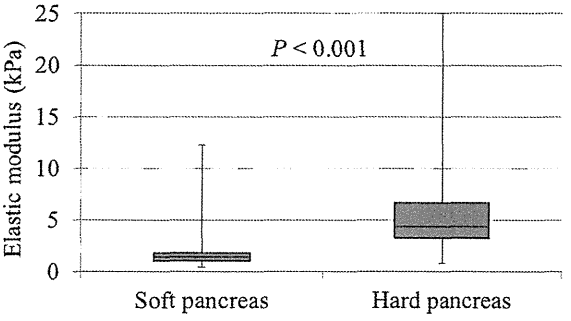

Fig 3. Correlation between elastic modulus and pancreatic consistency was evaluated using the Mann-Whitney *U*-test.

Correlation between EM and histologic findings. The EM was positively correlated with the ratio of azan positivity ($\rho = 0.381$, $P = .003$), the ratio of α-SMA positivity ($\rho = 0.369$, $P = .004$), and vessel density ($\rho = 0.559$, $P < .001$), and negatively correlated with lobular ratio ($\rho = -0.323$, $P = .013$). No correlation was observed between the EM and area of an entire cut surface ($\rho = 0.015$, $P = .910$), MPD ratio ($\rho = 0.175$, $P = .184$), or fat ratio ($\rho = 0.244$, $P = .062$).

Using the aforementioned EM cut-off value, we discovered the data for histologic parameters between EM values below and above 3.0 kPa as follows: azan positivity ratio, 6.5 ± 9.3% versus 14.2 ± 10.2% ($P = .003$); α-SMA positivity ratio, 5.8 ± 11.5% versus 14.1 ± 14.0% ($P = .006$); lobular ratio, 73.8 ± 18.7% versus 60.6 ± 16.0% ($P = .021$); vessel density, 1.4 ± 1.4/mm^2 versus 2.8 ± 1.5/mm^2 ($P < .001$) (Table).

Correlation between EM and occurrence of POPF. POPF occurred in 23 (International Study Group on Pancreatic Fistula Grade A in 11; Grade B in 11; Grade C in 1) of the 59 patients. The EM of the pancreas in cases without POPF was 3.5 ± 4.9 kPa, whereas that in cases associated

Table. Relationship between the EM with a cut-off at 3.0 kPa and histologic findings

	EM < 3.0 kPa	*EM > 3.0 kPa*	P *value*
Area of an entire cut surface, mm^2	250.1 ± 106.6	234.3 ± 82.3	.517
MPD ratio, %	0.168 ± 0.982	0.430 ± 1.140	.066
Azan-positive ratio, %	6.5 ± 9.3	14.2 ± 10.2	.003*
α-SMA-positive ratio, %	5.8 ± 11.5	14.1 ± 14.0	.006*
Lobular ratio, %	73.8 ± 18.7	60.6 ± 16.0	.021*
Fat ratio, %	15.4 ± 15.7	20.8 ± 12.4	.195
Vessel density,/mm^2	1.4 ± 1.4	2.8 ± 1.5	<.001*

*$P < .05$.
Relationship between EM with a cut-off at 3.0 kPa and histologic findings was evaluated using the Mann-Whitney *U*-test.
Azan, azan-Mallory; *EM*, elastic modulus; *MPD*, main pancreatic duct; *α-SMA*, α-smooth muscle actin.

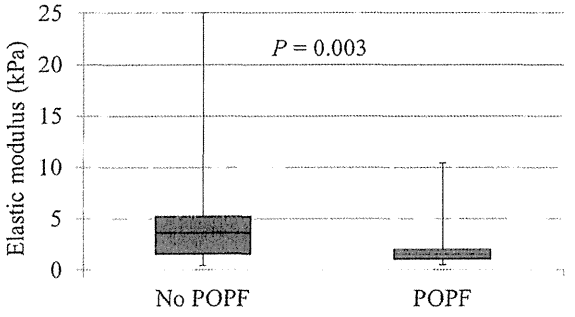

Fig 4. Correlation between elastic modulus and the occurrence of postoperative pancreatic fistula was evaluated using the Mann-Whitney *U*-test. *POPF*, Postoperative pancreatic fistula.

with POPF was 1.5 ± 2.0 kPa ($P = .003$) (Fig 4). Univariate logistic regression analysis showed that patients with an EM of less than 3.0 kPa had an increased risk of POPF with a hazard ratio of 9.333 (95% confidence interval 2.342–37.196; $P = .002$).

DISCUSSION

The present study has demonstrated for the first time that it is possible to measure the EM of a pancreatic cut edge objectively and quantitatively and that the value is strongly correlated with the tactile sensation felt by surgeons. The EM cut-off value of 3.0 kPa was a good clinical benchmark for tactile sensation and histological findings, as well as the occurrence of POPF after PD.

In surgery, a normal healthy pancreas generally is palpated intraoperatively as soft, whereas a diseased or inflamed pancreas often is palpated as hard. However, tactile assessment of the pancreas is an ill-defined issue, because it is performed only by skilled abdominal surgeons, and the intrinsic nature of pancreatic consistency has never been fully investigated. Detailed histologic examinations using computer-based morphometric image analysis[26,27] have revealed that the features associated with elevation of the EM of the pancreatic cut edge included an increased proportion of azan- and α-SMA-positive components, a decrease of lobules, and an increase of vessel density in the pancreatic parenchyma. The azan positivity ratio, as demonstrated by aniline blue staining, reflects the amount of collagen fibers and reticular fibers in the tissue,[28] and the α-SMA positivity ratio reflects the fibrotic response activated by myofibroblasts.[29,30] Increased vessel density represented by CD31 positivity, which showed a positive correlation with a greater EM, was considered to reflect neovascularization. Irreversible destruction of the exocrine parenchyma associated with fibrosis and neovascularization is a characteristic feature of chronic pancreatitis.[31,32] The data that have accumulated so far suggest that chronic inflammatory changes in the pancreatic parenchyma might result in the formation of a more tenacious pancreatic tissue structure associated with decreased secretion of pancreatic juice, and that this type of tissue may be better able to tolerate surgical suture placement, thus posing a lower risk of POPF after PD.

In a clinical setting, the measured EM value as an objective parameter of pancreatic consistency may facilitate a more definitive assessment of the risk of POPF after PD and may also allow meaningful comparisons among different institutions and studies, rather than subjective tactile sensation. Although there are no established reconstructive procedures or types of perioperative management to reduce the incidence of POPF after PD, countermeasures for a soft pancreas may differ from those for a hard pancreas because the former requires far more caution. Assessment of the EM may have potential to stratify patients according to the risk of POPF in prospective trials aimed at establishing definitive forms of patient care. Moreover, in the near future, accumulation of data

obtained by direct measurement of the EM of the pancreatic parenchyma may contribute to the preoperative assessment of pancreatic texture, POPF risk, and even lesion diagnosis, using elastographic imaging modalities.

The present study had certain limitations. First, the number of patients was relatively small. Second, although measurement of the EM was performed with an automatic indentation apparatus based on well-established physical rules,[6] reproducibility is an important consideration. The surface of the pancreas is not completely flat, and the aqueous component of interstitial tissue at the indentation point may disperse into the surrounding area. Physical characteristics that are not reflected in histologic features might create marked variability of data between cases. Moreover, the presence of plastic deformation and viscosity in the pancreatic specimen cannot be ruled out, and in fact this is a characteristic of human organs. Further accumulation of cases and validation with a modeling process may help to clarify how characteristics other than pure elasticity account for the properties of pancreatic tissue.

Third, although elevation of the EM was correlated with histologic findings such as chronic inflammation and a lower risk of POPF, pancreatic exocrine function was not investigated sufficiently. The relationships among fibrotic change, decrease of lobules, elevation of the EM, and exocrine function parameters should be the next focus of investigation. Furthermore, the utility of the EM for prediction of POPF was not evaluated adequately in this study. Because the EM of the pancreas showed a strong association with tactile sensation, multivariate predictive analysis for POPF including parameters possibly influencing each other could not be performed. A larger study will be needed to examine the value of the EM for prediction of POPF in comparison with other clinicopathologic parameters.

In conclusion, the present study has demonstrated that the EM of the cut edge of a resected pancreas represents the intraoperative tactile sensation felt by surgeons and reflects histologic findings including pancreatic fibrosis. The value of the EM also was correlated with the occurrence of POPF after PD. Measurement of the EM of the pancreas may facilitate an objective and quantitative assessment of pancreatic texture and a better understanding of the process of disease affecting the pancreatic parenchyma.

The authors wish to express special thanks to Toshio Ito of AXIOM Corporation for technical assistance with the Venustron device used for measurement of EM. Thanks are also extended to Prof. Subaru Kudo, Department of Science and Technology, Ishinomaki Senshu University, for his support with verification of the physical rules applied, and Kenta Okaya, Mitani Corporation, for support with image analysis of the histological specimens.

REFERENCES

1. Kawai M, Kondo S, Yamaue H, Wada K, Sano K, Motoi F, et al. Predictive risk factors for clinically relevant pancreatic fistula analyzed in 1,239 patients with pancreaticoduodenectomy: multicenter data collection as a project study of pancreatic surgery by the Japanese Society of Hepato-Biliary-Pancreatic Surgery. J Hepatobiliary Pancreat Sci 2011;18:601-8.
2. Hashimoto Y, Traverso LW. Incidence of pancreatic anastomotic failure and delayed gastric emptying after pancreatoduodenectomy in 507 consecutive patients: use of a web-based calculator to improve homogeneity of definition. Surgery 2010;147:503-15.
3. Ansorge C, Strömmer L, Andrén-Sandberg Å, Lundell L, Herrington MK, Segersvärd R. Structured intraoperative assessment of pancreatic gland characteristics in predicting complications after pancreaticoduodenectomy. Br J Surg 2012;99:1076-82.
4. Callery MP, Pratt WB, Kent TS, Chaikof EL, Vollmer CM Jr. A prospectively validated clinical risk score accurately predicts pancreatic fistula after pancreatoduodenectomy. J Am Coll Surg 2013;216:1-14.
5. Lin JW, Cameron JL, Yeo CJ, Riall TS, Lillemoe KD. Risk factors and outcomes in postpancreaticoduodenectomy pancreaticocutaneous fistula. J Gastrointest Surg 2004;8:951-9.
6. Feynman RP. Elasticity. In: Feynman RP, Leighton RB, Sands M, editors. The Feynman lectures on physics, Vol. 2. Reading, MA: Addison-Wesley; 1964. p. 2-12.
7. Pailler-Mattei C, Bec S, Zahouani H. In vivo measurements of the elastic mechanical properties of human skin by indentation tests. Med Eng Phys 2008;30:599-606.
8. Hara Y, Masuda Y, Hirao T, Yoshikawa N. The relationship between the Young's modulus of the stratum corneum and age: a pilot study. Skin Res Technol 2013;19:339-45.
9. Diridollou S, Vabre V, Berson M, Vaillant L, Black D, Lagarde JM, et al. Skin ageing: changes of physical properties of human skin in vivo. Int J Cosmet Sci 2001;23:353-62.
10. Tilleman TR, Tilleman MM, Neumann MH. The elastic properties of cancerous skin: Poisson's ratio and Young's modulus. Isr Med Assoc J 2004;6:753-5.
11. Leng H, Reyes MJ, Dong XN, Wang X. Effect of age on mechanical properties of the collagen phase in different orientations of human cortical bone. Bone 2013;55:288-91.
12. Samani A, Zubovits J, Plewes D. Elastic moduli of normal and pathological human breast tissues: an inversion-technique-based investigation of 169 samples. Phys Med Biol 2007;52:1565-76.
13. Kaster T, Sack I, Samani A. Measurement of the hyperelastic properties of ex vivo brain tissue slices. J Biomech 2011;44:1158-63.
14. Itoh Y, Itoh A, Kawashima H, Ohno E, Nakamura Y, Hiramatsu T, et al. Quantitative analysis of diagnosing pancreatic fibrosis using EUS-elastography (comparison with surgical specimens). J Gastroenterol [Epub ahead of print].

15. Doherty JR, Trahey GE, Nightingale KR, Palmeri ML. Acoustic radiation force elasticity imaging in diagnostic ultrasound. IEEE Trans Ultrason Ferroelectr Freq Control 2013;60:685-701.
16. D'Onofrio M, Crosara S, De Robertis R, Canestrini S, Demozzi E, Pozzi Mucelli R. Elastography of the pancreas. Eur J Radiol 2014; 83:415-9.
17. Iglesias-Garcia J, Domínguez-Muñoz JE, Castiñeira-Alvariño M, Luaces-Regueira M, Lariño-Noia J. Quantitative elastography associated with endoscopic ultrasound for the diagnosis of chronic pancreatitis. Endoscopy 2013;45:781-8.
18. Itokawa F, Itoi T, Sofuni A, Kurihara T, Tsuchiya T, Ishii K, et al. EUS elastography combined with the strain ratio of tissue elasticity for diagnosis of solid pancreatic masses. J Gastroenterol 2011;46:843-53.
19. Săftoiu A, Vilmann P, Gorunescu F, Janssen J, Hocke M, Larsen M, et al, European EUS Elastography Multicentric Study Group. Accuracy of endoscopic ultrasound elastography used for differential diagnosis of focal pancreatic masses: a multicenter study. Endoscopy 2011;43:596-603.
20. Sugimoto M, Takahashi S, Gotohda N, Kato Y, Kinoshita T, Shibasaki H, et al. Schematic pancreatic configuration: a risk assessment for postoperative pancreatic fistula after pancreaticoduodenectomy. J Gastrointest Surg 2013;17: 1744-51.
21. Bassi C, Dervenis C, Butturini G, Fingerhut A, Yeo C, Izbicki J, et al, International Study Group on Pancreatic Fistula Definition. Postoperative pancreatic fistula: an international study group (ISGPF) definition. Surgery 2005;138:8-13.
22. Hertz H. Über die Berührung fester elastischer Körper. Journal für die reine und angewandte Mathematik 1881; 92:156-71.
23. Polyakov P, Soussen C, Duan J, Duval JF, Brie D, Francius G. Automated force volume image processing for biological samples. PLoS One 2011;6:e18887.
24. Yamaoka H, Asato H, Ogasawara T, Nishizawa S, Takahashi T, Nakatsuka T, et al. Cartilage tissue engineering using human auricular chondrocytes embedded in different hydrogel materials. J Biomed Mater Res A 2006;78:1-11.
25. Choi AP, Zheng YP. Estimation of Young's modulus and Poisson's ratio of soft tissue from indentation using two different-sized indentors: finite element analysis of the finite deformation effect. Med Biol Eng Comput 2005;43:258-64.
26. Glozman T, Azhari H. A method for characterization of tissue elastic properties combining ultrasonic computed tomography with elastography. J Ultrasound Med 2010;29: 387-98.
27. Tsujino T, Seshimo I, Yamamoto H, Ngan CY, Ezumi K, Takemasa I, et al. Stromal myofibroblasts predict disease recurrence for colorectal cancer. Clin Cancer Res 2007;13: 2082-90.
28. Mallory FB. A contribution to staining methods. J Exp Med 1900;5:15-20.
29. Cherng S, Young J, Ma H. Alpha-smooth muscle actin (α-SMA). J Am Sci 2008;4:7-9.
30. Storch KN, Taatjes DJ, Bouffard NA, Locknar S, Bishop NM, Langevin HM. Alpha smooth muscle actin distribution in cytoplasm and nuclear invaginations of connective tissue fibroblasts. Histochem Cell Biol 2007;127:523-30.
31. Sarles H, Bernard JP, Johnson C. Pathogenesis and epidemiology of chronic pancreatitis. Annu Rev Med 1989;40:453-68.
32. Friess H, Malfertheiner P, Isenmann R, Kühne H, Beger HG, Büchler MW. The risk of pancreaticointestinal anastomosis can be predicted preoperatively. Pancreas 1996;13:202-8.

tumor-like lesions

腫瘍類似病変

疾患の概要

- 膵領域においては腫瘤を形成する腫瘍類似病変が存在し，腫瘍との鑑別が困難な症例がみられる．
- 腫瘍類似病変の代表的なものとしては，自己免疫性膵炎（autoimmune pancreatitis：AIP）と非自己免疫性慢性膵炎（non AIP chronic pancreatitis：non-AIP CP）がある（表1）．炎症性偽腫瘍の少なくとも一部は自己免疫性膵炎と考えられる．その他，過誤腫性病変や外傷性神経腫などの報告が散見されるが非常にまれである．
- 非自己免疫性慢性膵炎の多くはアルコール性であるが，特発性や遺伝性も少なからず存在する．自己免疫性膵炎は臨床病理学的に異なる1型，2型が存在するが，わが国においてはそのほとんどが1型である．
- 非自己免疫性慢性膵炎の2007年における新規発症患者数は15,200人，2002年の1年間における「自己免疫性膵炎臨床診断基準2006」に合致する患者数は953人であり，その一部は臨床的に腫瘍類似病変を呈すると思われる．海外からの報告では臨床的に腫瘍を疑われて手術された症例の16.6%，1996～2006年の国立がん研究センター東病院における手術症例では10.3%が腫瘍類似病変と考えられ，そのうち非自己免疫性慢性膵炎が53.3%，自己免疫性膵炎が46.7%であった．

臨床所見

好発年齢，性

- 非自己免疫性慢性膵炎は50～60代の男性に多くみられ，大酒家が多く，喫煙率が高い．
- 1型自己免疫性膵炎はやや高齢の60～70代の男性に好発し，飲酒歴を有さないことが多い．
- 2型自己免疫性膵炎は欧米に多く，わが国ではきわめて少ない．1型と比較して若年者に多く，炎症性腸疾患の合併率が高い．

臨床症状

- 非自己免疫性慢性膵炎においては上腹部痛，腰背部痛を呈することが多く，嘔気・嘔吐，腹部膨満感や全身倦怠感などがみられる．病態が進行すると膵機能の低下により，脂肪便，体重減少や糖尿病による症状が出現する．
- 自己免疫性膵炎では強い腹痛を認めることは少なく，軽い心窩部痛程度が多い．

表1 自己免疫性膵炎臨床診断基準 2011

A. 診断項目	
Ⅰ．膵腫大	a. びまん性腫大（diffuse） b. 限局性腫大（segmental/focal）
Ⅱ．主膵管の不整狭細像	ERP
Ⅲ．血清学的所見	高 IgG4 血症（≧ 135mg/dL）
Ⅳ．病理所見 右の所見のうち a. ３つ以上を認める b. ２つを認める	①高度のリンパ球，形質細胞の浸潤と，線維化 ②強拡１視野当たり 10 個を超える IgG4 陽性形質細胞浸潤 ③花むしろ状線維化（storiform fibrosis） ④閉塞性静脈炎（obliterative phlebitis）
Ⅴ．膵外病変 硬化性胆管炎 硬化性涙腺炎・唾液腺炎 後腹膜線維症	a. 臨床的病変 臨床所見および画像所見において，膵外胆管の硬化性胆管炎，硬化性涙腺炎・唾液腺炎（Mikulicz 病）あるいは後腹膜線維症と診断できる． b. 病理学的病変 硬化性胆管炎，硬化性涙腺炎・唾液腺炎，後腹膜線維症の特徴的な病理所見を認める．

〈オプション〉ステロイド治療の効果

専門施設においては，膵癌や胆管癌を除外後に，ステロイドによる治療効果を診断項目に含むこともできる．

悪性疾患の鑑別が難しい場合は超音波内視鏡下穿刺吸引（EUS-FNA）細胞診まで行っておくことが望ましいが，病理学的な悪性腫瘍の除外診断なく，ステロイド投与による安易な治療的診断は避けるべきである．

B. 診断	
Ⅰ．確診	①びまん型：Ⅰa+〈Ⅲ/Ⅳb/Ⅴ(a/b)〉 ②限局型：Ⅰb+Ⅱ+〈Ⅲ/Ⅳb/Ⅴ(a+b)〉の２つ以上 または　Ⅰb+Ⅱ+〈Ⅲ/Ⅳb/Ⅴ(a/b)〉+オプション ③病理組織学的確診：Ⅳa
Ⅱ．準確診	限局型：Ⅰb+Ⅱ+〈Ⅲ/Ⅳb/Ⅴ(a+b)〉
Ⅲ．疑診*	びまん型：Ⅰa+Ⅱ+オプション 限局型：Ⅰb+Ⅱ+オプション

自己免疫性膵炎を示唆する限局性膵腫大を呈する例で ERP 像が得られなかった場合，EUS-FNA で膵癌が除外され，Ⅲ/Ⅳb/Ⅴ（a+b）の１つ以上を満たせば，疑診とする．さらに，オプション所見が追加されれば準確診とする．

疑診*：わが国ではきわめてまれな２型の可能性もある．+；かつ，/；または

（日本膵臓学会・厚生労働省難治性膵疾患に関する調査研究班．報告　自己免疫性膵炎臨床診断基準 2011．膵臓 2012；27：19 より抜粋）

約半数に閉塞性黄疸が出現する．また，しばしば涙腺炎や後腹膜線維症を合併する．

画像所見

- 非自己免疫性慢性膵炎では，膵管内の結石および膵全体に分布する複数ないしびまん性の石灰化を認める．
- 自己免疫性膵炎ではびまん性あるいは限局性の膵腫大が特徴的であり，主膵管の拡張は伴わないことが多い．限局性病変や非典型的な症例においては膵癌との鑑別が困難なことがある．

血液生化学所見

- 非自己免疫性慢性膵炎において血中膵酵素の上昇が特徴である．
- 自己免疫性膵炎における膵酵素上昇の頻度は低いが，血清γグロブリン，IgG，IgG4，抗核抗体，リウマトイド因子の上昇が高頻度でみられる．２型では IgG4 上昇率が低い．